Available online at www.sciencedirect.com
ScienceDirect
J. Mater. Sci. Technol., 2012, **28**(10), 905–912.
JMST
www.JMST.org

Corrosion Evolution of Reinforcing Steel in Concrete under Dry/Wet Cyclic Conditions Contaminated with Chloride

J. Wei, X.X. Fu, J.H. Dong† *and W. Ke*
State Key Laboratory of Corrosion and Protection, Institute of Metal Research, Chinese Academy of Sciences, Shenyang 110016, China

[Manuscript received May 13, 2011, in revised form July 16, 2011]

The corrosion evolution of rebar in concrete was monitored by electrochemical impedance spectroscopy (EIS) under dry/wet alternated accelerated corrosion test. Four stages with different dynamic characteristics were observed during the corrosion evolution. They were passive stage, local corrosion controlled by the charge transfer step, accelerated corrosion controlled by the mass transfer step, and constant rate corrosion controlled by the mass transfer step through a barrier layer. X-ray diffraction (XRD) analysis showed that the corrosion product of rebar in mortar was composed of α-FeOOH, γ-FeOOH and Fe_3O_4. The corrosion mechanisms of all four stages were discussed and the corrosion reactions were proposed according to the corrosion product and corrosion evolution characteristics.

KEY WORDS: Rebar; Concrete; Electrochemical impedance spectroscopy (EIS); Corrosion evolution

1. Introduction

It is well known that corrosion of reinforcing steel bar (rebar) is the most important cause of concrete degradation. The rebar is initially in passive state due to the formation of passive film on its surface in the high alkaline condition (pH value 12.5–13.5) of the pore solution in concrete[1]. However, the passive film can be destroyed by aggressive mediums (such as chloride, sulfate) or by an acidification of the environment near the rebar (carbonation)[2,3]. Once the passive film is destroyed, the corrosion will be initiated and proceed, which will induce continuously forming and accumulating of rust on the rebar surface. It has been known that a mass of accumulated rust may lead to a powerful internal expansion force which has two breakage effects on the concrete structure[4,5]. First, the expansion force can crack the concrete structure. Second, it may extrude the rust out of the concrete along the seam between the rebar and the concrete, and thus reduce the binding force between the rebar and the concrete.

The corrosion of rebar in concrete is a complicated process. Although some studies have focused on the corrosion of rebar in concrete, the corrosion evolution of rebar in concrete, especially the corrosion dynamic characteristics from initial passivation to a thick rust layer covered state is not fully known up to now[6]. It will be very helpful to monitor the corrosion evolution of rebar in concrete for understanding the corrosion mechanism, evaluating the corroded extent and predicting the service life of reinforced concrete structure. Among a lot of electrochemical measuring techniques, electrochemical impedance spectroscopy (EIS) has been proved to be a powerful tool for monitoring the corrosion process of rebar in concrete[7,8]. It provides not only the electrochemical dynamic information which reflects passivation, charge transfer step and mass transfer step of the electrode process, but also the resistance and the dielectrical properties of the surface film on rebar. Because the service life of reinforced concrete is usually from several decades to hundreds of years, the corrosion of rebar in concrete is very slow. Therefore, it is necessary to accelerate the corrosion process in laboratory investigations.

† Corresponding author. Ph.D.; Tel.: +86 24 23915912; Fax: +86 24 23894149; E-mail address: jhdong@imr.ac.cn. (J.H. Dong).

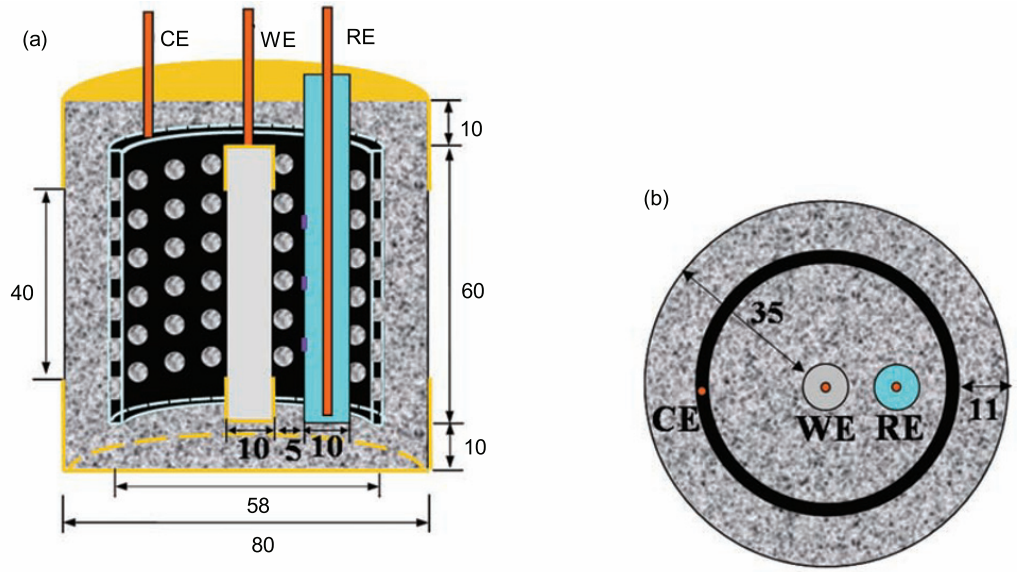

Fig. 1 Schematic diagrams of the electrode system for reinforced mortar samples: (a) side sectional view, (b) top sectional view (unit: mm)

The aim of this paper is to study the corrosion evolution of rebar in concrete by employing EIS method under the dry/wet alternated accelerated corrosion environment contaminated with chloride. Equivalent circuit (EC) models were used to interpret the dynamic characteristics during the corrosion evolution of rebar in concrete.

2. Experimental

2.1 Material and procedures

2.1.1 Rebar samples preparation

The steel used in the experiment is a commercial 20SiMn hot-rolled rebar. The chemical composition (wt%) is: C 0.17–0.25, Si 0.40–0.80, Mn 1.20–1.60, P 0.050, S 0.050. The as-received rebar samples were machined into cylinders of Φ10 mm×60 mm, and the surfaces were polished using 1200# SiC paper.

2.1.2 Mortar samples preparation

Reinforced mortar samples (Φ80 mm×80 mm) were cast according to the standard experimental procedures using ordinary Portland cement 42.5 (with a water/cement ratio of 0.5 and cement/sand ratio of 1/3). The schematic diagram of the mortar samples is shown in Fig. 1. Demoulded after casting for 24 h, the mortar samples were cured in a standard curing chamber at 20±1 °C and ≥95% RH (relative humidity) for 28 d. In order to avoid the non-uniform penetration of solution, both ends of the mortar samples were coated with epoxy resin leaving 40 mm height profile exposed. Three parallel samples were prepared in the experiment to ensure the repeatability.

2.1.3 Electrode system design

A three-electrode cell was used for the electrochemical measurement in this experiment, as shown in Fig. 1. The working electrode (WE) was the machined rebar samples. Both ends of the rebar were coated with dense epoxy, leaving an exposed length of 40 mm. The rebar was positioned at the center of the mortar sample with a cover thickness of 35 mm. The reference electrode (RE) was $Cu/CuSO_4$ electrode which was positioned 5 mm near the working electrode to decrease the current-resistance (IR) drop between WE and RE. In order to distribute the electrical signal uniformly, a 60 mm height annular graphite electrode was used as the counter electrode (CE), which was positioned in the mortar with the cover thickness of 11 mm.

2.2 Dry/wet cyclic accelerated corrosion tests

Before the dry/wet cyclic tests, the samples were immersed in de-ionized water for 1 d which was referred as cycle 0. Then, 14 cycles of severe dry/wet cyclic corrosion tests were carried out to accelerate the corrosion of rebar in mortar. During each cycle, the samples are dried at 80 °C for 4 d in a drying cabinet and then immersed in 3.5% NaCl solution (25 °C) for 1 d. Both of the drying and immersing processes can make the mortar samples reach constant weight.

2.3 Electrochemical measurement

After each dry/wet cycle, the corrosion potential (E_{corr}) and EIS were measured when the mortar samples were immersed in 3.5% NaCl solution, using a PAR 273 potentiostat and a PAR 5210E lock-in amplifier. EIS measurements were performed at the open-circuit potential with a 10 mV perturbation from 100 kHz to 10 mHz. All the measurements were

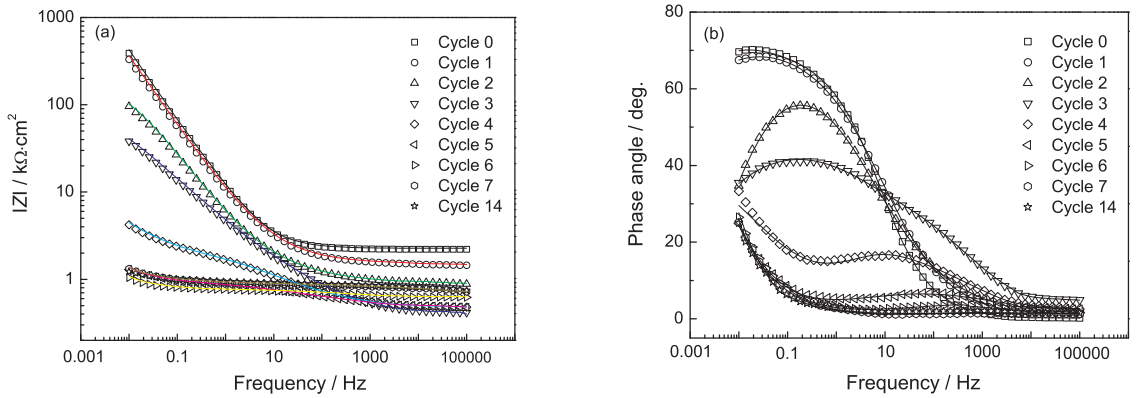

Fig. 2 (a) Bode |Z| plot and (b) Bode phase plot of rebar in mortar for cycles 1–7 and 14, solid lines represent the fitting results

carried out at room temperature (25 °C). The EIS results were fitted by ZSimpWin software based on the equivalent circuit models.

2.4 Morphology observation

After 14 cycles of dry/wet cyclic accelerated corrosion tests, the cross-section morphology of the rust layer was observed using scanning electronic microscopy (SEM, HITACHI S3400N). The preparing process of the samples for cross-section morphology was as follows: first, the samples with the size of Φ15 mm×15 mm cut from the rusted rebar were mounted using epoxy resin to fix the rust layer; then, they were grinded and polished using kerosene as the lubricant; finally, they were cleaned by ultrasonic in alcohol and then dried.

2.5 X-ray diffraction (XRD) analysis

To analyze the compositions of the corrosion product, XRD experiment was carried out using a Rigaku-D/max 2000 diffractometer by employing a Cu target under 50 kV and 250 mA. The scan rate was 2 °C/min. The powder sample used for XRD analysis was prepared by grinding the corrosion products scraped from the rebar surface.

3. Results and Discussion

3.1 Evolution of the EIS spectra

Fig. 2 shows the Bode plots of rebar in mortar after each cycle of the dry/wet alternated accelerated corrosion test. The $|Z|$ plot shows that the $|Z|$ value at low frequency decays quickly from cycle 2 to 6, and the difference becomes negligible after cycle 6. And the $|Z|$ value of high frequency decreases before cycle 3 and then increases to a constant value. The phase angle plot shows that the peak value of the phase angle is high at low frequency in the initial cycle 0 and 1, and then it drops and shifts toward the middle frequency with the increase of the cycles. Since cycle 4, the phase angle generates a smearing at low frequency region. After cycle 6, the peak value of phase angle in the middle frequency decays to a minimum value. The difference of the phase angle plot after cycle 6 becomes negligible. These results indicate that the corrosion of rebar undergoes complicated evolution processes and shows different corrosion dynamic characteristics during the dry/wet cycles[9,10].

3.2 EC models for fitting the EIS results

According to the evolution characteristics of the EIS spectra of the rebar in concrete during the dry/wet cyclic corrosion test, four physical models of the rebar/mortar interface and corresponding equivalent circuit (EC) models were proposed to fit the EIS data, as shown in Fig. 3.

In the initial cycle 0 and 1, the total impedance of rebar specimen is high, and the phase angle at low frequency reaches the peak and then keeps horizontal. Under this condition, the rebar is in passive state. Fig. 3(a) describes the physical model and EC model of stage when the rebar is in passive state. In the concrete system, film capacitance and double electric layer capacitance usually deviate from pure capacitance due to the dispersion effect, and the constant phase element (CPE) is used instead of pure capacitance[11–13]. The equation of CPE is shown as follows:

$$Z_{\mathrm{Q}} = \frac{1}{Y_0} \cdot (j\omega)^{-n} \tag{1}$$

where Z_{Q} represents the impedance of CPE, Y_0 represents the admittance of CPE, n represents the dispersion power of CPE, ω represents the angular frequency, $j{=}(-1)^{1/2}$.

In the EC model, R_{s} stands for the solution resistance of mortar pores between RE and WE, R_{f} stands for the resistance of the passive film, Q_{f} stands for the CPE of the passive film, R_{ct} stands for the charge transfer resistance, and Q_{dl} stands for the CPE of the double electric layer.

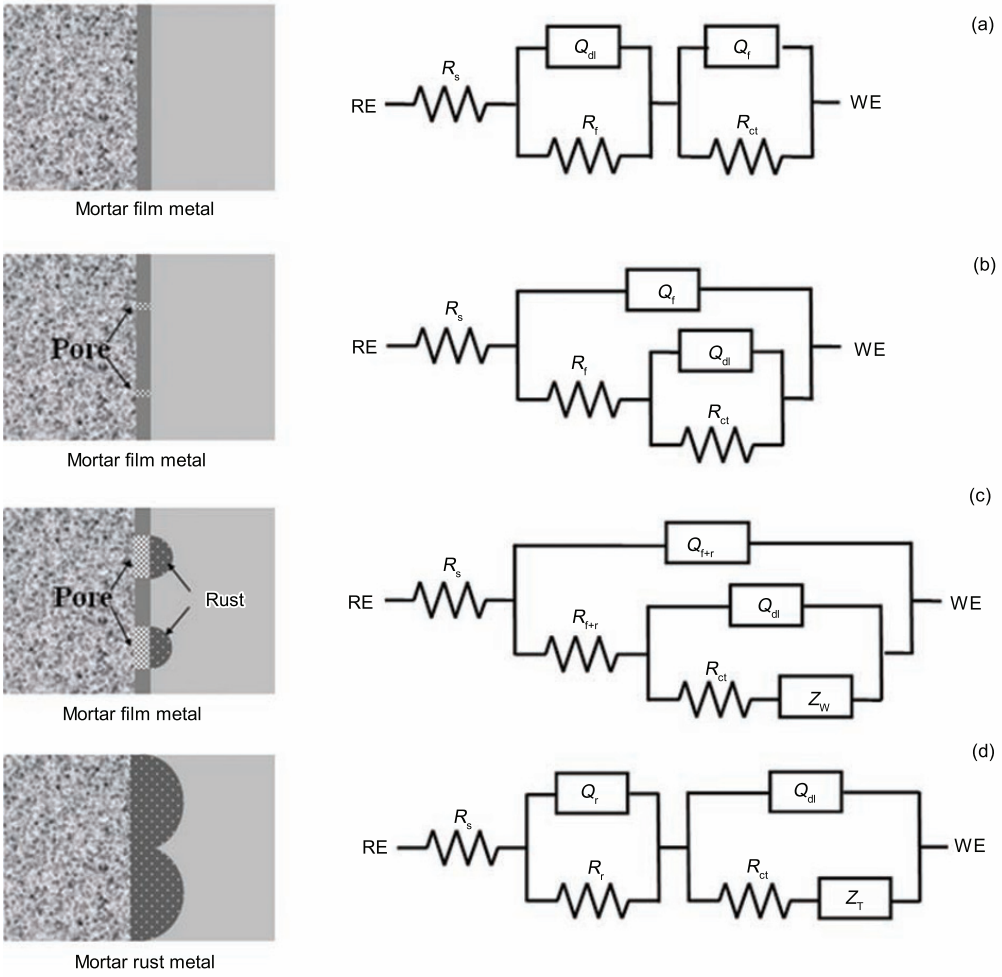

Fig. 3 Physical models and the corresponding EC for four stages: (a) stage I, (b) stage II, (c) stage III, (d) stage IV

With increasing dry/wet cycles, the total impedance decreases and the phase angle at low frequency drops after reaching the peak since cycle 2. These results indicate that the passive film is locally destroyed by the aggressive ions, and the corrosion cell forms with the exposed rebar substrate acting as anode and the undamaged film acting as cathode when electrolyte is existing. Fig. 3(b) describes the physical model and EC model of stage II (cycles 2 and 3). Stage II corresponds to the state at which the local corrosion occurs and the rate-controlled step of corrosion process is the charge transfer step.

As for the EIS spectra after cycle 4, the phase angle plots present a smearing at low frequency region, which indicates that the mass transfer behavior occurs on the rebar/concrete interface[14]. Fig. 3(c) describes the physical model and EC model of stage III (cycles 4 and 5). Stage III corresponds to the state at which the rate of charge transfer increases and the diffusion step becomes slow step of the electrode process. In the EC model, R_{f+r} stands for the sum resistance of the passive film and the rust, Q_{f+r} stands for the sum CPE of the passive film and the rust, and Z_W[15] stands for the Warburg resistance of the semi-infinite diffusion process.

With the development of the corrosion process, a thick rust layer forms on the rebar surface which may block the diffusion of reactants and products to the rebar surface and from the rebar surface. Fig. 3(d) describes the physical model and EC model of stage IV (cycles 6–14). Stage IV corresponds to the state at which the electrode process is controlled by the diffusion process through a barrier layer. In the EC model, R_r is the resistance of rust layer; Q_r is the capacitance of the rust layer; Z_T is the barrier layer diffusion resistance[16].

3.3 Fitting results of EIS spectra

The fitting curves of the EIS results are presented in Fig. 2 as the solid lines for each spectrum, and the fitting parameters are listed in Table 1. All the resistances of R_f, R_{f+r} and R_r are expressed as R_1, and the constant phase element of Q_f, Q_{f+r} and Q_r are expressed as Q_1.

R_s decreases in the early several cycles and then

Table 1 Fitting results of EIS data of rebar

Cycle	R_s /kΩ·cm^2	Q_1-Y$_0$×10^4 /Ω^{-1}·cm^{-2}·s$^{-n_1}$	n_1	R_1 /kΩ·cm^2	Q_{dl}-Y$_0$×10^4 /Ω^{-1}·cm^{-2}·s$^{-n_{dl}}$	
0	2.20	1.40	0.63	5.39	0.24	
1	1.47	1.48	0.45	4.99	0.27	
2	0.94	2.33	0.70	1.31	0.58	
3	0.41	2.91	0.60	1.21	0.63	
4	0.47	2.16	0.52	0.72	6.27	
5	0.44	3.36	0.36	0.54	85.95	
6	0.58	3.38	0.37	0.19	134.2	
7	0.71	9.62	0.19	0.28	94.32	
14	0.70	7.29	0.19	0.30	117.8	
Cycle	n_{dl}	R_{ct} /kΩ·cm^2	Z_W-Y$_0$×10^4 /Ω^{-1}·cm^{-2}·s$^{-0.5}$	Z_T-Y$_0$×10^4 /Ω^{-1}·cm^{-2}·s$^{-0.5}$	Z_T-B /s$^{-0.5}$	$\chi^2 \times 10^4$
0	0.81	9679	–	–	–	0.67
1	0.80	5466	–	–	–	0.21
2	0.71	187.7	–	–	–	2.86
3	0.50	55.2	–	–	–	0.25
4	0.63	1.47	12.89	–	–	3.37
5	0.77	0.21	17.18	–	–	1.10
6	0.83	0.11	–	25.97	4.31	2.66
7	0.73	0.12	–	16.11	4.43	0.37
14	0.78	0.11	–	12.85	4.22	2.00

increases in the latter cycles. It correlates to the accumulation of salt transmitted to the mortar. The decrease of R_s is caused by the continuous penetration and deposition of NaCl into the mortar during the early dry/wet cycles. The penetrated NaCl saturates the pore solution at cycle 3, and R_s changes little from cycle 3 to 5. After that, some of the corrosion product fills in the pores of the mortar, which resists the transmitting of the penetrated ions and results in the increase of R_s.

The decrease of R_1 with the increase of the cycles indicates that the passive film is destroyed by the penetrated Cl^-. It decays to the minimum at cycle 6, and then it gradually increases with the accumulation of the corrosion product. The capacitance of Q_1-Y$_0$ also increases with the cycles, which indicates that the permeability of the film or rust increases and more corrosive ions can reach the rebar substrate. Furthermore, R_{ct} decreases to the minimum at cycle 6, and then keeps a constant value. It indicates that the corrosion rate of rebar increases with increasing dry/wet cycles, and the rebar is corroded at a constant rate after cycle 6.

The corrosion current density of rebar can be calculated according to the Stern–Geary equation:

$$I_{corr} = B/R_{ct} \quad (2)$$

where I_{corr} represents the corrosion current density and B represents the Stern–Geary constant. The values of 52 and 26 mV are often used in the calculation of B for the bare steel in the passive and active states, respectively[17,18]. Therefore, in this work, the value of 52 mV was used to calculate the I_{corr} of cycles 0 and 1, and the value of 26 mV was used for the other cycles. Fig. 4 shows the evolution of I_{corr} with the cycles. According to the criteria for estimating the corrosion of reinforcing steel[19], the rebar is in passive condition when I_{corr}<0.1 μA·cm^{-2}; the corrosion extent of rebar is low to moderate when 0.1<I_{corr}<0.5 μA·cm^{-2}; the corrosion extent of rebar is moderate to high when 0.5<I_{corr}<1.0 μA·cm^{-2}; the corrosion extent of rebar is high when I_{corr}>1.0 μA·cm^{-2}. It is therefore verified by the value of corrosion rate that the rebar is in passive state in stage I. The corrosion rate of rebar in stage II is relatively slow. The corrosion rate of rebar in stage III is high, and it keeps stable during stage IV.

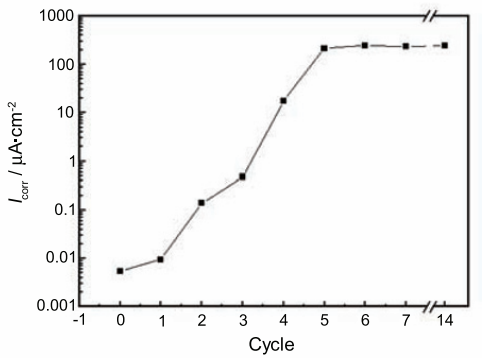

Fig. 4 Evolution of I_{corr} of rebar with dry/wet cycles

3.4 Evolution of E_{corr} of the rebar in concrete

Fig. 5 shows the evolution of E_{corr} with dry/wet cycles, which was measured after each dry/wet cycle

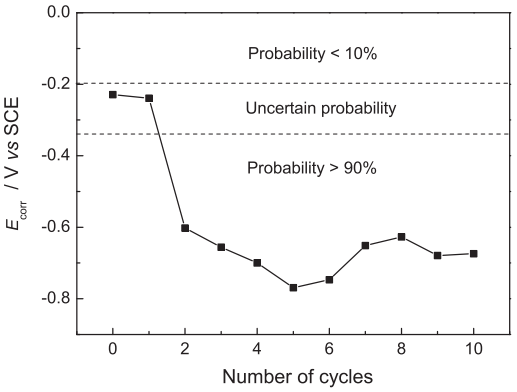

Fig. 5 Evolution of $E_{\rm corr}$ with dry/wet cycles

when the mortar was immersed in NaCl solution. The ASTM C876 standard[20] has determined three $E_{\rm corr}$ levels to identify the corrosion probability of rebar in concrete. That is, when $E_{\rm corr}$ (vs SCE)>-0.20 V, the corroded probability of rebar in concrete is less than 10%; when $E_{\rm corr}$ (vs SCE)<-0.35 V, the corroded probability of rebar in concrete is more than 90%; when it locates in the middle region, the probability is uncertain. Therefore, when the rebar in concrete remained at passive state at cycles 0 and 1, $E_{\rm corr}$ located in the region where corrosion probability was uncertain. After that, it dropped to the region where corrosion probability was more than 90%.

3.5 Morphology of corrosion products

Fig. 6 shows the cross-section morphologies of corrosion product after 14 cycles of dry/wet alternated accelerated corrosion tests. It is shown that the corrosion product contains an inner layer and an outer layer. The inner layer of dark gray looks loose and porous, and the outer layer of light gray looks compact. The thickness of the rust layer is in the order of 10^2 μm, and it is not uniform. For instance, Fig. 6(a) indicates a local rust position with a thickness of 440 μm, whereas Fig. 6(b) shows most of the rust area with a thickness of 220 μm. This non-uniform distribution of corrosion depth implies that the local corrosion occurs on the rebar.

3.6 Compositions of corrosion product

The compositions of corrosion products of rebar are shown in Fig. 7. The phases of Fe, NaCl and SiO_2 in the XRD pattern are introduced from rebar substrate and the environment system of mortar during the sample preparation. Thus, the corrosion products of rebar are composed of γ-FeOOH, Fe_3O_4 and α-FeOOH.

4. Discussion

According to the EIS results, the corrosion evolution process of rebar in mortar includes four stages during the 14 cycles of dry/wet alternated corrosion test.

During the curing period, two processes occur simultaneously on the surface of bare rebar in the chloride free mortar: the active anode dissolution and the passivation of rebar[21]. The initial step of both two processes is the adsorption process of OH^- on rebar surface, as expressed by reaction (3). After the formation of the intermediate product of $(FeOH)_{ad}$, the active anode dissolution and the passivation continue to take place according to the following reactions (4) and (5) and reactions (6) and (7), respectively. The reaction rates of these two processes determine the transformation of surface state of rebar in mortar. If the anode dissolution rate is faster than the passivation rate, the rebar will dissolute continuously. Otherwise, if the passivation rate is faster than the anode dissolution rate, the area of passivation on the rebar surface will increase continuously, and eventually a complete passive film will form on the whole surface of rebar.

Adsorption process:

$$\mathrm{Fe} + \mathrm{OH}^- \leftrightarrow (\mathrm{FeOH})_{\rm ad} + e^- \tag{3}$$

Anode dissolution:

$$(\mathrm{FeOH})_{\rm ad} \rightarrow \mathrm{FeOH}^+ + e^- \tag{4}$$

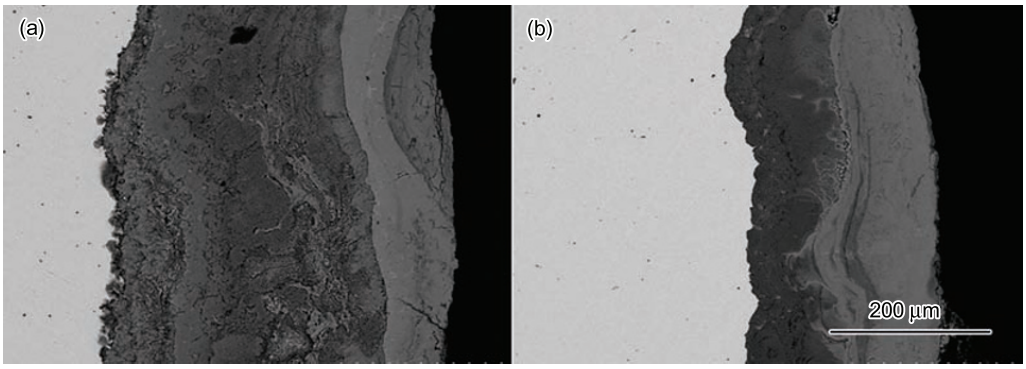

Fig. 6 Cross-section morphologies of corrosion products: (a) local regions, (b) most regions

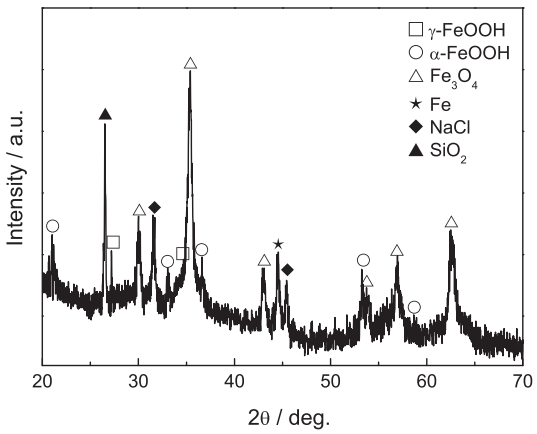

Fig. 7 Compositions of corrosion products of rebar

$$FeOH^+ \leftrightarrow Fe^{2+} + OH^- \quad (5)$$

Passivation:

$$(FeOH)_{ad} + OH^- \leftrightarrow [Fe(OH)_2]_{ad} + e^- \quad (6)$$

$$[Fe(OH)_2]_{ad} + OH^- \rightarrow FeOOH + H_2O + e^- \quad (7)$$

In the high alkaline condition (pH value 12.5–13.5) of the pore solution in mortar, the high OH^- content slows the reaction rate of reaction (5) and accelerates the passivation reactions (6) and (7). Therefore, a layer of passive film forms on the rebar surface which can protect the rebar against corrosion.

According to the results from EIS and E_{corr}, the rebar keeps in passive state before cycle 1. In cycle 1, although the Cl^- had transmitted to the interface of rebar/concrete after immersion in 3.5% NaCl solution for 1 d, the rebar still maintained in passive state as the breakdown of the passive film induced by Cl^- needs an incubation period[22,23]. In stage II, the passive film on the rebar surface keeps intact and compact which suppresses the electron transfer of electrochemical reactions.

In stage II, the content of Cl^- on some local regions of film surface reached the threshold content for destroying the passive film. When some local regions of the passive film are destroyed, the corrosion cell forms when oxygen exists. The locally exposed rebar substrate acts as anode and the large area of undamaged film acts as cathode. The anode reactions are shown in (8)–(11), and the cathode reaction is the reduction of oxygen, as shown in reaction (12)[24]. The Cl^- does not be consumed in the corrosion reactions. Moreover, the Cl^- plays the role of depolarization at anode. This action accelerates the corrosion process. Therefore, R_f, R_{ct} and E_{corr} decrease significantly since cycle 2. However, the corrosion rate is relatively slow in stage II (I_{corr}<1 $\mu A \cdot cm^{-2}$), and the dissolved oxygen in the pore solution is sufficient for charge transfer reduction. Therefore, the corrosion process is controlled by charge transfer step.

Anode reactions:

$$Fe \rightarrow Fe^{2+} + 2e^- \quad (8)$$

$$Fe^{2+} + Cl^- \rightarrow [FeCl_{complex}]^+ \quad (9)$$

$$[FeCl_{complex}]^+ + 2OH^- \rightarrow Fe(OH)_2 + Cl^- \quad (10)$$

$$Fe(OH)_2 + OH^- \rightarrow FeOOH + H_2O + e^- \quad (11)$$

Cathode reaction:

$$H_2O + 1/2O_2 + 2e^- \rightarrow 2OH^- \quad (12)$$

In stage III, along with the corrosion proceeding, some corrosion products form on the anode region. The volume expansion caused by corrosion products enlarges the broken area of the passive film, which aggravates the corrosion of rebar. Furthermore, when the corrosion product FeOOH exists on the rebar surface, the reduction of FeOOH shown as reaction (13) will happen prior to the reduction of oxygen at the cathode[25]. As this reaction can proceed without oxygen being consumed, and it can consume Fe^{2+} and FeOOH, the anode dissolution reactions will be promoted. Therefore, the I_{corr} increases rapidly with increasing cycles. With the increase of the corrosion rate and the formation of the corrosion product on the rebar surface, the diffusion of the reactants and products cannot satisfy the need of electrode reaction. Therefore, the rate-controlled step of corrosion process will change from the charge transfer step to the diffusion step.

Cathode reaction:

$$Fe^{2+} + 8FeOOH + 2e^- \rightarrow 3Fe_3O_4 + 4H_2O \quad (13)$$

In stage IV, with the expansion of the depth and width of the corrosion pits and the increase of the rust thickness, the whole passive film is destroyed. When a thick rust layer forms on the rebar surface, the diffusion process that the reactants reach the rebar surface and the products leave the rebar surface becomes especially difficult. Therefore, after cycle 6, the rate-controlled step of corrosion process is the diffusion process through a barrier layer. However, despite the formation of the thick rust layer can restrict the rapid increase of the corrosion rate, it cannot reduce the corrosion rate. Moreover, as Fe_3O_4 is not the most stable rust product, it will transform to α-FeOOH according to reaction (14) if the duration is long enough. Therefore, the corrosion products consist of γ-FeOOH, Fe_3O_4 and α-FeOOH. Furthermore, according to the cross-section morphologies of corrosion products, as shown in Fig. 6, the corrosion products can be divided into two layers. The inner layer is loose and porous, while the outer layer is more compact than the inner layer. As the initial corrosion product is γ-FeOOH which has inherent loose structure, the inner layer of rust is probably composed of γ-FeOOH. Comparing with γ-FeOOH, the structures of Fe_3O_4 and α-FeOOH are more compact. Therefore, the outer layer of rust is probably composed of Fe_3O_4 and α-FeOOH which are the subsequent reaction products as shown in reactions (13) and (14).

$$Fe_3O_4 + H_2O + OH^- \rightarrow 3\alpha\text{-FeOOH} + e^- \quad (14)$$

5. Conclusion

The local corrosion occurs on rebar in chloride contaminated mortar. The corrosion evolution process of rebar includes four stages. Those are, passive stage, local corrosion controlled by the charge transfer step, accelerated corrosion controlled by the mass transfer step, and constant rate corrosion controlled by the mass transfer step through a barrier layer. The corrosion products of rebar in mortar consists of γ-FeOOH, Fe_3O_4 and α-FeOOH. The corrosion products can be divided into two layers. The inner layer is loose and porous, which is probably composed of γ-FeOOH. However, the outer layer is more compact than the inner layer, which is probably composed of Fe_3O_4 and α-FeOOH.

REFERENCES

[1] B.B. Hope and A.K.C. Ip: *ACI Mater. J.*, 1987, **84**, 306.
[2] M. Moreno, W. Moms and M.G. Alvarez: *Corros. Sci.*, 2004, **46**, 2681.
[3] W. Aperador, R. Mejía de Gutiérrez and D.M. Bastidas: *Corros. Sci.*, 2009, **51**, 2027.
[4] R. Vera, M. Villarroel, A.M. Carvajal, E. Vera and C. Ortiz: *Mater. Chem. Phys.*, 2009, **114**, 467.
[5] S. Guzmán, J.C. Gálvez and J.M. Sancho: *Cement Concrete Res.*, 2011, **41**, 893.
[6] M.F. Montemor, A.M.P. Simões and M.G.S. Ferreira: *Cement Concrete Compd.*, 2003, **25**, 491.
[7] M. Sanchez, J. Gregori and C. Alonso: *Electrochim. Acta*, 2007, **52**, 7634.
[8] D.H Leila and T. Ezzedine: *Cement Concrete Res.*, 1996, **26**, 253.
[9] C. Liu, Q. Bi, A. Leyland and A. Matthews: *Corros. Sci.*, 2003, **45**, 1257.
[10] J.Q. Zhang and C.N. Cao: *J. Chin. Soc. Corros. Protect.*, 1998, **19**, 99.
[11] G.F. Qiao and J.P. Ou: *Electrochim. Acta*, 2007, **52**, 8008.
[12] V. Feliu and J.A. Gonzalez: *Corros. Sci.*, 1998, **40**, 975.
[13] V. Kolluru, Subramaniam and M.D. Bi: *Corros. Sci*, 2009, **51**, 1976.
[14] J. Flis, H.W. Pickering and K. Osseo-Asare: *Electrochim. Acta*, 1998, **43**, 1921.
[15] A. Amirudin and D. Thierry: *Prog. Org. Coat.*, 1995, **26**, 1.
[16] C.N. Cao and J.Q. Zhang: *Introduction of Electrochemical Impedance Spectra*, 2nd edn, Science Press, Beijing, 2002, 117. (in Chinese)
[17] C. Andrade and J.A. Gonzalez: *Mater. Corros.*, 1978, **29**, 515.
[18] J.A. Gonzalez and C. Andrade: *Br. Corros. J.*, 1982, **17**, 21.
[19] S.G. Millard, K.R. Gowers and Js. Gill: *American Concrete Institute SP 128*, ed V.M. Malhotra, Detroit, 1991, 373.
[20] ASTM C876-91, Standard Test Method for Half-Cell Potentials of Uncoated Reinforcing Steel in Concrete[S].
[21] C.N. Cao: *Principles of Corrosion Electrochemistry*, Chemistry Industry Press, Beijing, 2004, 261. (in Chinese)
[22] O. Poupard, A. Aït-Mokhtar and P. Dumargue: *Cement Concrete Res.*, 2004, **34**, 991.
[23] M. Saremi and E. Mahallati: *Cement Concrete Res.*, 2002, **32**, 1915.
[24] J. Balma, D. Darwin, J.P. Browning and C.E. Locke: *Structural Engineering and Engineering Materials*, The University of Kansas Center for Research, 2002, 6.
[25] I. Suzuki, N. Masuko and Y Hisamatsu: *Corros. Sci.*, 1979, **19**, 521.